

# 16 New Transiting Planet Candidates from *Kepler* Q1-Q6 Data

X.Huang<sup>1\*</sup>, G.Á.Bakos<sup>1,2</sup>, J.D.Hartman<sup>1</sup>

<sup>1</sup> Department of Astrophysical Sciences, 4 Ivy Lane, Peyton Hall, Princeton University, Princeton, NJ 08544

<sup>2</sup> Alfred P. Sloan Research Fellow

20 November 2018

## ABSTRACT

We have performed an extensive search for planet candidates in the publicly available *Kepler* Long Cadence data from quarters Q1 through Q6. The search method consists of initial de-trending of the data, applying the trend filtering algorithm, searching for transit signals with the Box Least Squares fitting method in two frequency domains, visual inspection of the potential transit candidates, and in-depth analysis of the shortlisted candidates. In this paper we present 16 new periodic planet candidates and 8 single transit events. The periods of these planet candidates vary from  $\sim 0.968$  day to  $\sim 440$  day. Nine of the planet candidates have radii smaller than  $3 R_{\oplus}$ . We also report seven newly identified false positives—systems that look like transiting planets, but are probably due to blended eclipsing binaries.

**Key words:** planetary systems-stars: individual (KIC 3345675, KIC 3346154, KIC 4150804, KIC 5008501, KIC 5128673, KIC 5437945, KIC 5563300, KIC 5689351, KIC 5965819, KIC 6047072, KIC 6699368, KIC 6805414, KIC 7899070, KIC 8552719)

## 1 INTRODUCTION

The field of transiting extrasolar planets (TEPs) has exploded over the past few years. One major contributor is the *Kepler Space Mission*, continuously monitoring 156000 stars in a  $115 \text{ deg}^2$  field (Borucki et al. 2010; Koch et al. 2010). Since its launch in 2009, it has found 2321 planetary transit candidates<sup>1</sup> (Borucki et al. 2011a; Batalha et al. 2012). The first 4 months of data (Q1 and Q2) yielded 1235 planet candidates associated with 997 host stars, including 60 confirmed planets around 33 stars (Borucki et al. (2011b), hereafter B11). The *Kepler* team has developed increasingly sophisticated procedures to identify planet candidates (Smith et al. 2012) and multiple systems (Steffen et al. 2012; Ford et al. 2012). Using more data (16 months) and improved detection procedures, the total number of planet candidates has almost doubled since the release by B11 (Batalha et al. (2012), hereafter B12).

An independent search with different tools can build confidence in the reliability of the detections, and the completeness of the sample, by e.g. providing new candidates that were missed by the *Kepler* science team. One such effort is the citizen science initiative, called PlanetHunters (Fischer et al. 2012; Lintott et al. 2012), based on the idea of Zooniverse (Lintott et al. 2008). Making use of human eyes

to search for transit like events through a user friendly computer interface, 6 planet candidates were identified. These were then subjected to the vetting procedure of the *Kepler* team, and four of them survived this process, i.e. they are not false alarms, as much as it can be determined from the *Kepler* data. However, conducting a visual search of all the raw light curves takes a lot of human effort. Quoted from Fischer et al. (2012): “It is impractical for a single individual to review each of the  $\sim 150,000$  light curves in every quarterly release of the *Kepler* data base.” While challenging, it is certainly feasible for an individual to examine  $\sim 150,000$  light curves, especially if sophisticated computer algorithms narrow down the list to a somewhat smaller sample of candidate transits that can be then checked very carefully. Also, note that small planets are often hard to recover by visual inspection without phase-folding the light curve at the suspected periodicity of the signal.

Encouraged by these observations, we started an independent search for transiting planet candidates in *Kepler*’s long-cadence data. *Kepler* observations are grouped into so-called quarters (each having a duration of 3 months, except for Q0 and Q1, which are shorter). At the end of each quarter, the spacecraft rotates 90 degrees, to adjust its solar panels. The majority of *Kepler* stars are observed as long cadence (LC) targets, for which data are obtained by gathering over 270 exposures within 29.4 min; 512 stars are also observed in short cadence (SC) mode with 58.9 s intervals (Jenkins et al. 2010b; Gilliland et al. 2010; Murphy 2012).

\* E-mail: xuhuang@princeton.edu;

<sup>1</sup> <http://kepler.nasa.gov/Mission/discoveries/candidates/>

We used quarters Q0-Q6 in this search, which data were released to the public in Jan 2012. Our methodology is based on our experience conducting a similar search with HATNet (Bakos et al. 2004), a wide-field ground-based survey. Broadly speaking, the *Kepler* space-based data is of much higher quality than any ground-based data. Ground based observations often exhibit large gaps in the time-series, either due to the rotation of the Earth, or inclement weather conditions. The data quality is highly variable due to changing extinction, clouds, background, seeing, etc. The per-point photometric precision is typically worse than from space, partly because of the above effects of ground-based observations, and partly due to the use of inexpensive hardware (e.g. front illuminated CCDs).

Altogether, our ground-based data is of lower signal-to-noise, has inhomogeneous quality, and exhibits complex systematic variations with long gaps. For example, not a single transit event has been found in HATNet data by direct visual inspection; transits are detected through sophisticated data mining and phase-folding. Consequently, tools developed for a transit search using ground based data may be very efficient in recovering transit signals from *Kepler*.

In this paper we employ tools from the transit detection pipeline of the HATNet project, after sufficient modifications to conform to the *Kepler* data. We also develop a pre-filtering method that corrects the *Kepler* light curves for known anomalies and systematics, before searching them for transit events. Our search is blind in the sense that the list of *Kepler* candidates was not consulted during the search. The large majority of our candidates have already been identified by *Kepler* team. We report 16 new planet candidates and 8 *single* transit events that haven't been assigned as KOIs (Kepler Objects of Interests).

The structure of the paper is as follows. The data processing methodology is discussed in §2, the generation of the final candidate list and the modeling of candidates are laid out in §3, and the candidates are exhibited in §4.

## 2 DATA ANALYSIS

### 2.1 Removal of points and long trend filtering

We make use of the *Kepler* public LC light curves. We begin with the TIME and SAP\_FLUX (raw flux) columns in the FITS files. The raw flux is already corrected for cosmic rays and background variations by the *Kepler* team (Jenkins et al. 2010a). First we convert the fluxes to magnitudes and set the mean value for each star to its *Kepler* magnitude taken from the Kepler Input Catalog (KIC)<sup>2</sup>.

The second step is to clean the light curves based on the data anomalies table in the *Kepler Data Release Notes* for each quarter (Christiansen et al. 2012,b; Machalek et al. 2010, 2011). We summarize all the important events in Q1 through Q6 in Table 1. We also describe the definition of anomaly types (adopted from *Kepler Data Characteristic Hand Book*) and our methods of correction for each type in the table notations. Generally, for data anomalies involving a discontinuity we model the jump by a polynomial with an offset in magnitude after the gap. The fitting uses 50 points

on both sides around the gap. The offset is then subtracted from the data after the jump. In the time range during safe modes (Q2 and Q4), or earth point recoveries (Q3, Q4 and Q6), there is an exponential decay in the flux. We identify and remove the whole exponential decay rather than attempting to correct for the effect.

Most of the stars exhibit long-term trends. We follow the traditional high pass filter method (Ahmed et al. 1974; Maze & Faigler 2010), and apply a cosine filter on all the cleaned light curves. For each light curve, before computing the filter, we generate a model by applying a 100 point ( $\sim 2$  day long) median filter. This is done to prevent distortions due to outlier points (including introducing spurious “transit” signals). The cosine filter is then computed as the sum of a linear component and  $N = T_{total}/\Delta T$  cosine functions, where the highest frequency is  $1/\Delta T$  ( $\Delta T = 10$  day), and  $T_{total}$  is the total time span of the light curve:

$$M(t_j) = a \frac{(t_j - t_s)}{T_{total}} + \sum_{i=0, N} b_i \cos \left[ i\pi \frac{(t_j - t_s)}{T_{total}} \right]. \quad (1)$$

Here  $t_j$  is the time of the  $j$ th measurement, and  $t_s$  is the first time instance in the light curve. The coefficient  $a$  for the linear component and coefficient  $b_i$  for the  $i$ th cosine functions are computed by a least squares fitting procedure on the model. The fitted trend  $M(t_j)$  is then subtracted from the light curves. We combine the long trend filtered light curves from Q1-Q6 by offsetting the magnitude of all the quarters referring to the magnitude of Q1.

### 2.2 Sky groups and Systematic Trend filtering

Following the long-term trend filtering procedure described above (§ 2.1), we then apply the Trend Filtering Algorithm (TFA) developed by Kovács et al. (2005) on the combined (Q1-Q6) light curves. The idea of TFA is to select a set of template light curves, which we assume to contain information of the systematic variations, and then construct a linear filter based on their shared time-series for each light curve to be corrected. TFA can remove systematic variations that are either shorter time-scale than those corrected by the cosine filter, or have an arbitrary functional form that is not well described by the sum of cosine functions. TFA assumes that the light curves are sampled at the same time-instances.

To construct a set of template light curves with the same time-base, we make use of the sky group information provided by the *Kepler* team. The sky group number is defined as the CCD channel number on which the stars fell during Q2 of the *Kepler* operation. *Kepler* has 21 modules. Each module contains 2 CCD chips and each CCD contains 2 output channels. The focal plane rotates 90 degrees when the telescope switches to a new quarter every 3 months, except for the initial transition between quarters Q0 to Q1. Generally, the stars that belong to the same sky group share the same CCD channel all the time, although this channel changes from time to time. Therefore, each sky group shares the same time base, and has similar instrumental systematic trends. Additionally, stars in the same sky group are related in terms of their sky position, so that the local variabilities (e.g. local background variations or flux contamination from nearby stars) are often shared. TFA is designed to reduce this kind of general (shared by a number of stars) systematics.

<sup>2</sup> <http://tdc-www.harvard.edu/software/catalogs/kic.html>

We construct a separate filter for each sky group, selecting  $\sim 300$  template light curves in each case. Template stars are selected randomly, but in a manner that ensures a uniform distribution of their positions across the field. To exclude variable stars, we also impose a constraint on their median deviation around the median magnitudes (MAD, a quantity that is insensitive to outliers); stars with high MAD are ruled out from the templates. The total number of data points (time samples) in each template time base is  $\sim 17000 - 22000$ , depending on the total length of time series in the sky group. In other words, we are not overfitting the light curves.

Altogether 124840 stars in 84 sky groups were selected and analyzed with TFA from the *Kepler* public LC data. For each sky group, we only selected stars that have been observed during the complete time range, and have not been affected by the failure of module 3. This is because the TFA analysis requires the same time-base to generate the filter per sky group. Module 3 failed in the middle of Q4, while observing sky groups 5, 6, 7 and 8. Due to the rotation of spacecraft, the Q5 data in sky groups 49, 50, 51 and 52, and the Q6 data in sky groups 77, 78, 79, and 80 were not available. Stars in these sky groups are still included if they have a complete data set in other quarters. Otherwise, we only selected light curves containing all the Q1-Q6 data (which has a total observation time of  $\sim 500$  days).

We note that the *Kepler* team has recently implemented a new “cotrending” algorithm, called PDC-MAP (Smith et al. 2012). This algorithm uses 16 Cotrending Basis Vectors (CBV) that are generated by a singular value decomposition method applied separately to each channel and each quarter. This method has some commonalities with TFA. We did not make use of the PDC-MAP data, since it was not available for the Q1-Q6 data when we started our analysis.

In Figure 1 we demonstrate our filtering process on the a randomly selected light curve (KIC 003346154). The great improvement by the procedure is clearly demonstrated.

### 2.3 Box Least Square Fitting (BLS) and Transit Analysis

We use the box least square fitting algorithm (Kovács et al. 2002) to search for periodic transit signals in the TFA filtered light curves. In order to maximize the efficiency of the BLS search in a wide frequency range, we divide the frequency search into two, only slightly overlapping frequency domains; one with  $0.02 \text{ d}^{-1} < f_1 < 1.0 \text{ d}^{-1}$  and the other with  $0.004 \text{ d}^{-1} < f_2 < 0.03 \text{ d}^{-1}$ . We use a different number of frequency steps and BLS bins in each domain. We use the SNR (signal to noise ratio, measured in the BLS spectrum) and DSP (dip significance) parameters (for details, see Kovács et al. 2002) of the first five frequency peaks reported by BLS to select candidate transit signals for manual inspection.

We adopt selection threshold of 9 and 7.6 (8.5 and 7.0) for SNR and DSP in the first (second) frequency domain, respectively. These are not optimized selection criteria, but instead ensure that no shallow or rare transit events are missed. The low detection threshold also means that events will require close visual inspection. With the above limit, we

selected 82200 stars to fold with the five best BLS reported periods and manually inspected all the folded light curves.

Transit-like features in the folded light curves are flagged and further examined in the visual inspection. We reject light curves with recognizable depth variation for odd and even peaks and also those with depths indicating very large planetary radii ( $R_p > 2R_J$ ). For the transits visible in the unfolded light curves, we directly inspect the shape and transit center of each transit; for the transits invisible in the unfolded light curves (due to low S/N), we perform phase-folding with the BLS-detected frequency before examining the data.

## 3 RESULTS

### 3.1 Generation of the planet candidate short list

We flagged 1503 stars as possible transiting planet hosts during manual inspection. Among them, we found 266 stars which are categorized as eclipsing binaries (EB)<sup>3</sup> (Prša et al. 2011), and 166 stars which are listed as false positives (FP)<sup>4</sup> (Borucki et al. 2011b) by the *Kepler* team. We also cross-matched our results with the KOI catalog<sup>5</sup> (Borucki et al. 2011a,b; Batalha et al. 2012), and found that we recovered 811 of the 908 planetary systems reported by B11 (here we only count the systems in our LC light curve samples). Our recovery statistics with respect to the B12 candidate list is worse; we found only 71 of the 630 additional planetary systems by our detection procedure. We think that part of the reason is the imperfect correction of certain short period variable stars, leading to residual red noise which masks the shallow transits. We are still refining our filtering procedure to enhance the performance. A more detailed report on the statistics and our detection efficiency will be reported later. Here we focus on the discovery of the new planet candidates which were not reported by either B11 or B12.

We examined in detail the remaining candidates which are not included in the publicly available lists of candidates, EBs, or FPs. We re-applied the cosine filter to these light curves constructed with a greater number of cosine functions and a smaller frequency interval. We aimed to clean systematic variations from the light curves (whether intrinsic to the stars, or due to instrumental effects), leaving flat light curves with transits. The cosine functions are generated in a frequency range adjusted according to the visual determination of the frequency of the stellar variation. To preserve the transit signal, we applied a median filter with a window width at least twice that of the detected transit duration, before generating the cosine filter. BLS was applied again on the corrected light curves. The first ten peaks in the BLS spectrum are examined and compared to the previous detection, ensuring the detection of transit signal is robust. As shown below in §3.2, all candidates were checked against false positive scenarios.

<sup>3</sup> [http://archive.stsci.edu/kepler/eclipsing\\_binaries.html](http://archive.stsci.edu/kepler/eclipsing_binaries.html)

<sup>4</sup> [http://archive.stsci.edu/kepler/false\\_positives.html](http://archive.stsci.edu/kepler/false_positives.html)

<sup>5</sup> [http://archive.stsci.edu/kepler/planet\\_candidates.html](http://archive.stsci.edu/kepler/planet_candidates.html)

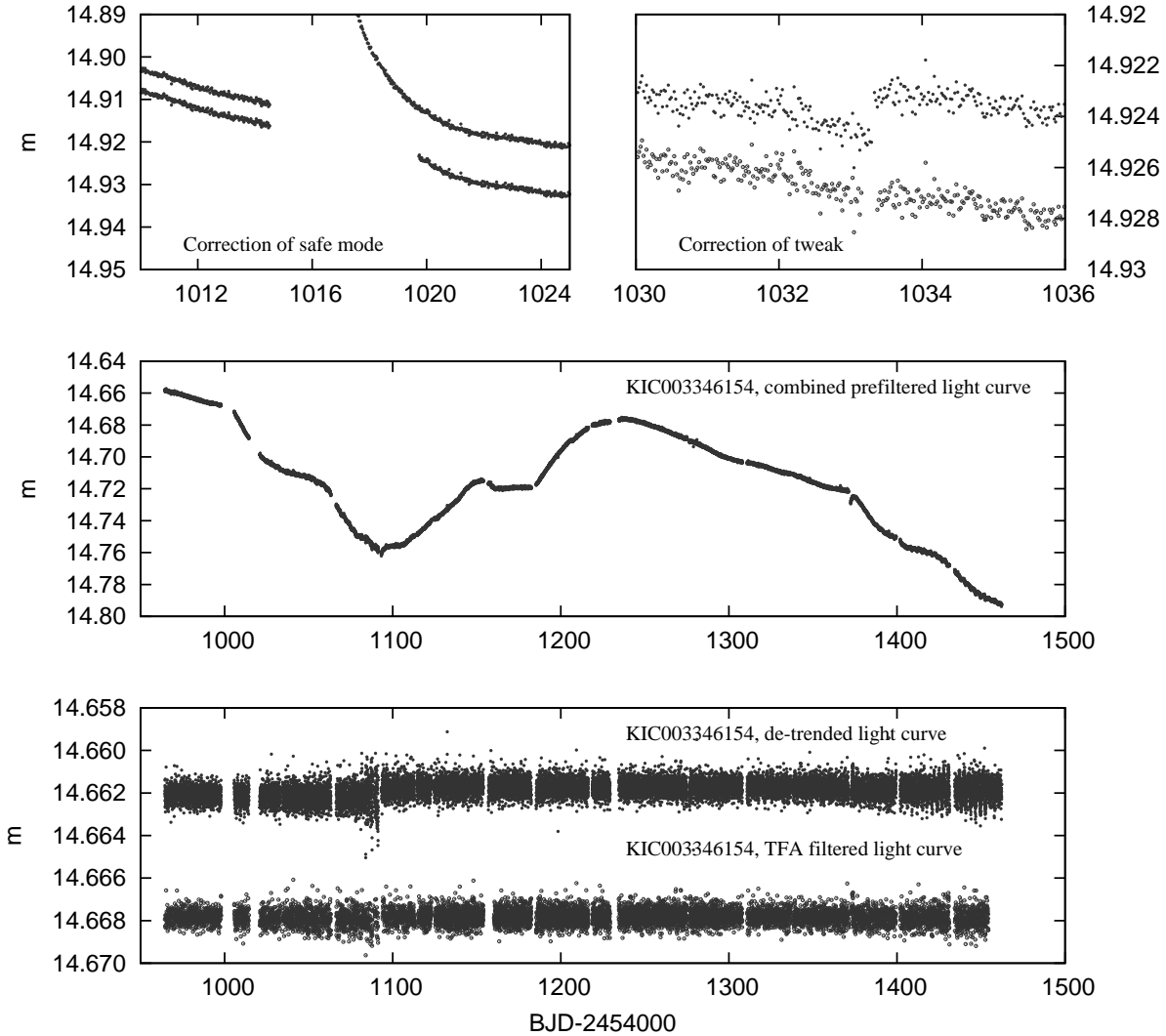


**Figure 1.** An example of filtering process for the light curve of KIC 003346154. The ordinate is in the units of approximate *Kepler* magnitude: Top panel: correction of safe mode (left) and tweak (right), (the example is taken from Q2). The corrected light curve is plotted below the uncorrected one. Middle panel: combined light curve from Q1-Q6 after pre-filtering process, i.e. correction of anomaly data points and combine the light curves from all the quarters. Bottom panel: light curve after long trend filtering (solid symbols) and after TFA (empty circles).

### 3.2 False positive detection and robustness checking

We use the moment-derived centroids provided by the *Kepler* FITS files to further eliminate possible FPs. For long period planet candidates, we visually examine the centroids at the transit time. For short period planet candidates, we examine the phase-folded centroid curves (de-trended by the cosine filter). We present one of our “failed” transit candidates as an example in Figure 2. The folded light curve would naively suggest that there is a transit signal due to a planet with  $R_p/R_\star = 0.0198 \pm 0.0017$  and period of  $P = 2.00783 \pm 3.8 \times 10^{-5}$  day. However, the phased centroids

show a shift of  $\sim 0.004$  pixels in the  $y$  direction during transit events, which indicates this is likely to be a false positive signal due to a blended eclipsing binary. According to the 2MASS image stamp, there is no nearby source within an area of  $20'' \times 20''$ , i.e. the binary is not resolved in the 2MASS images. We provide a list of seven false positives flagged by this method in Table 2. These stars have not been reported by the *Kepler* team in their false positive lists. The stellar information and estimated shifts in both directions are also given in our table.

We also used the public target pixel files and PyKE

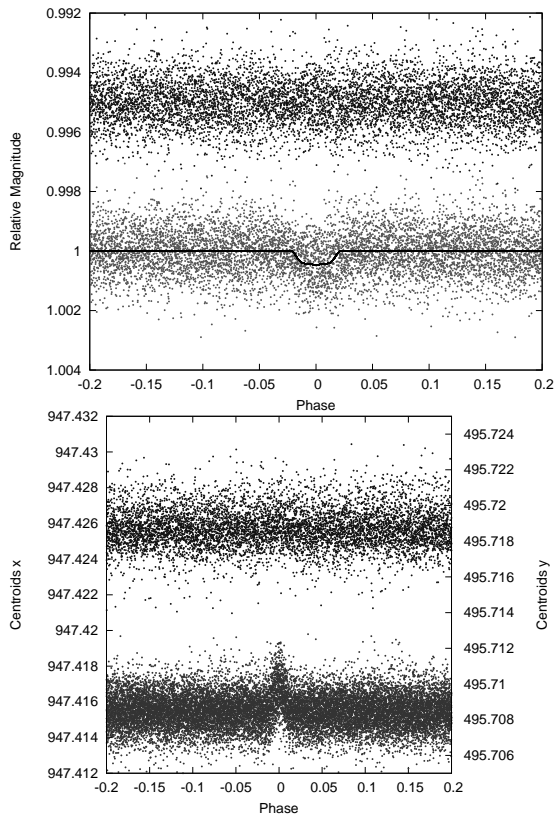


**Figure 2.** Light curves and centroids for KIC 004072333, phase-folded using the detected period and epoch. Top panel: phase-folded light curve with period  $P = 2.00783$  days and  $E = 2455302.8774$  (BJD). Bottom panel: folded centroids in the  $x$  direction (top and grey) and the  $y$  direction (bottom and dark) with the same parameters. This detection is flagged as a false positive due to the shift of centroids in the  $y$  direction during transit. There is no visible companion in the 2MASS image stamp within  $20'' \times 20''$  for this particular star.

package<sup>6</sup> developed by the *Kepler* team, to obtain pixel light curves for all of our candidates with transit depth greater than 1 mmag. This encompasses 8 planet candidates and 5 single transit events. It is difficult to perform the same analysis on shallower transits, because of the low signal-to-noise of the events in the light curves of individual pixels.

Here we take one of our new detections, KIC 005437945, as an example for our photometry analysis. We detected 4 non-periodic transit events altogether, which could be explained as due to two long period planet candidates with different epochs, depths and durations. The transits in Q1 and Q6 are due to a  $P \approx 440$  day planet candidate; and the transits in Q2 and Q5 are due to a  $P \approx 220$  day planet candidate (i.e. they are in a 2:1 resonance). We present the analysis for the transit event in Q6 here. We show the pixel image of out-of-transit, in-transit and the difference imaging in Figure 3. The images are computed by plotting the mean out-of-transit flux ( $\pm 2$  day around the transit events), the mean in-transit flux and the difference between the two. The difference imaging during transit is identical to the out-

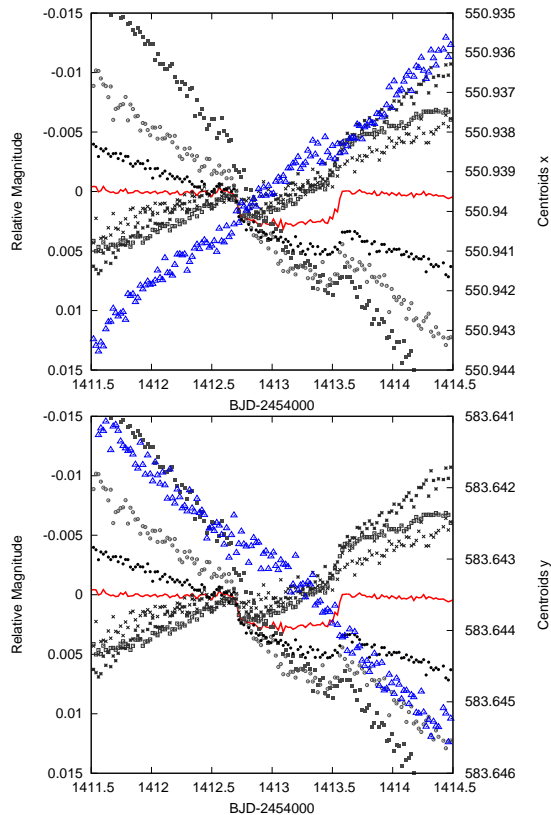


**Figure 4.** Red solid line: light curve flux for transit events in Q6 for KIC 005437945. Blue and triangles: raw centroids  $x$  (top panel) and  $y$  (bottom panel). Different types of black points: light curves generated from different pixels separately in the aperture using keprextract from the PyKE package.

of-transit flux distribution. No obvious background source is indicated for this particular star.

We further use the pixel calibration technique enabled by PyKE to extract light curves from every single pixel in the aperture. Figure 4 shows the light curves extracted separately from 6 pixels in the Q6 aperture (the aperture is shown in Figure 3). We can see that while the magnitude in every single pixel changes during the transit, they all show visible evidence for the transit event with roughly the same depth. The averaged flux from all the pixels has a flat out-of-transit magnitude. In addition, the centroids do not present an anomalous shift during the transit events.

For the rest of transits which are not suitable for applying the single pixel analysis, we use other methods to at least ensure the robustness of the detection. We removed the detected transit signal according to the epoch, period and transit duration reported by BLS. Then we computed six different BLS spectra for each of the new light curves. The BLS spectra were obtained with 3 different sets of parameters (different frequency steps and bin numbers), each set of parameters are used twice. The first 10 peaks of every BLS spectrum were analyzed. We compared these 60 frequency peaks to our original transit detections. For all of the 8 planetary transit signals we analyzed, the original periods as well as their harmonics were not detected in the transit-removed light curves.

Altogether 16 planet candidates entered our final list

<sup>6</sup> <http://keplergo.arc.nasa.gov/ContributedSoftwarePyKEP.shtml>

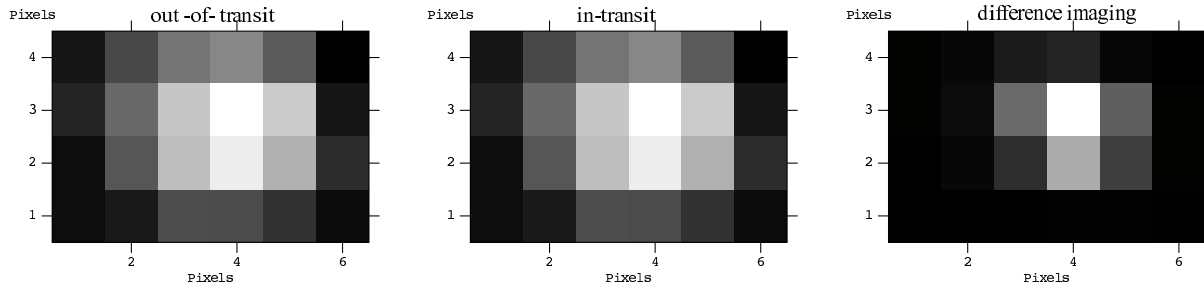


**Figure 3.** Out-of-transit image (in log scale of flux), in-transit image (in log scale of flux) and the difference between the two (in linear scale of flux) from the pixel files for KIC 005437945 Q6 transit. We do not see a visible shift in the flux distribution on the pixel image during transit, demonstrating that the apparent transit is not due to a variation of a background source.

of new detections. The properties of their host stars are provided in Table 3. The detected periods range from  $\sim 0.968$  day to  $\sim 440$  day. We also found 2 new multiple systems, each with two planet candidates. One of the planet candidates we found is a third transit signal in KOI 505, which is already known as a multiple system, hosting 2 KOIs.

We also include 8 *single* transit events. Two of these single transit events are around KOI stars with a known planet candidate. If the single transits were confirmed to both be planets, both systems would be re-classified as multiple systems. Using the convention of Batalha et al. (2012) for single transit events, we assign a negative integer period number for these potential candidates. We compute the minimum allowed period according to the given time span of the light curve and the epoch of transit. This is taken as the estimated period for single transit events in modeling.

### 3.3 Analysis

The transit modeling of all the candidates is based only on the *Kepler* light curves and the stellar parameters provided by the KIC. The parameters we can obtain directly from light curves are the transit depths, durations, ingress/egress durations, and individual transit centers.

Without radial velocity (RV) data, mass determinations for these systems are generally not available. It may be possible to measure the masses through subtle photometric effects, like ellipsoidal variations and relativistic beaming (Mazeh & Faigler 2010; Kipping & Spiegel 2011). These effects are prominent for close binary stellar systems as well as massive planet companions (Loeb & Gaudi 2003). We did not observe these effects in our candidates.

The eccentricity is also unknown, although broad limits can be placed on the orbital configuration for very wide transits (Kipping 2008). An eccentric orbit could result in asymmetry in the transit light curves, as well as a shift in the mid-time of transits relative to the occultation events. In principle, the eccentricity could also be derived from modeling the detailed shape of a transit light curve. However, detecting these effects requires extremely high resolution and SNR light curves, which were not available for our candidates. Generally speaking, we observe no apparent asymmetry in any of our candidates, which suggests modest eccentricity or certain values of argument of periastron. We assume circular orbits in our modeling, following the convention of previous KOI modeling with only transit light curve information (Batalha et al. 2012).

We assume no flux dilution from blended nearby stars in our modeling. This is plausible for most our candidates. We inspect the 2MASS image stamps with an area of  $20'' \times 20''$  centered on each target. Four of them have nearby companions, which are marked out in Table 4.

In theory, one could also fit for the limb darkening coefficients, but this requires very high signal-to-noise and well sampled data, i.e. deep transits or many transit events (Kipping & Bakos 2011). We use a quadratic limb darkening formalism to model the transit light curves. The limb darkening coefficients (LDC) corresponding to the stellar atmospheres are interpolated with the stellar parameters from KIC in the ATLAS model grid LDCs provided by Sing (2010) for *Kepler*. The stellar parameters and the LDCs for the candidates are listed in Table 3. We also generate a grid of 1000 randomly selected stars from KIC with known stellar parameters and the interpolated their LDCs following the method described above. We then use these to determine LDCs for stars without information such as  $T_{\text{eff}}$ ,  $\log g$  and  $[\text{Fe}/\text{H}]$  by linear interpolating in the J, H, K color space. Since the LDCs obtained with this method have larger uncertainties, the derived planet parameters for planets without host star parameters provided by KIC should be treated with caution.

To conclude, in our transit modeling, we do not fit for:

- the planet mass  $M_p$ ;
- the eccentricity  $e$  of the orbit, which is assumed to be zero;
- the blending due to nearby stars, which is set to be zero;
- the LDCs of stars, which are computed as described above.

We modelled the following geometric parameters which correspond:

- the fractional planet radius  $R_p/R_*$ ;
- the square of the impact parameter square  $b^2$ ;
- the inverse of half duration  $\zeta/R_* = 2/T_{dur}$ . This quality is related to  $a/R_*$  for zero eccentricity via the relation:

$$\frac{\zeta}{R_*} = \frac{a}{R_*} \frac{2\pi}{P} \frac{1}{\sqrt{1-b^2}}. \quad (2)$$

In the fitting procedure we constrained the quantities  $b^2, R_p/R_*, \zeta/R_*$  to be the same for each individual transit for a selected candidate.

We also fitted for the additional parameters of out-of-transit magnitudes and transit centers. For the short period cases (with more than 100 transits in the light curve), we fit the median out-of-transit magnitude, first transit center  $T_A$  and the last transit center  $T_B$  as free parameters, with the

total number of transits  $N$  fixed. We also assume that the transits are strictly periodic. We do not model the out-of-transit variation; the light curve is assumed to be flat. For our long period candidates (with less than 10 transits in the light curve), we use a slightly different method. We take the out-of-transit magnitude and transit centers of individual transits as independent parameters, the total number of free parameters in the fit for a  $N$  transit light curve is  $2N+3$ . The candidates with only a single transit observed were fitted as if they were an individual transit in a long period system with a rough lower limit on the period.

In the fitting we used the formalism of Mandel & Agol (2002), and the methodology laid out in the analysis of HATNet planet discoveries (Bakos et al. 2010). A 10000 step Markov Chain Monte Carlo (MCMC) simulation is then applied around the best fitting parameters to explore the parameter space. The final reported planet parameters and estimated errors are taken as the median and median deviation of all the accepted jumps in the chain. The period is then recalculated by taking the median of  $(T_B - T_A)/N$  for all the accepted jumps in the chain. We derive the transit number closest to the average of  $T_A$  and  $T_B$  (weighted by their errors as derived from the MCMC runs), and use the transit center of this transit (calculated from  $T_A, T_B, N$ ) as optimal epoch.

We summarize the planet parameters for all the candidates in Table 4. The best fitted model on the phase folded light curves and the residuals from the best fitted model are presented in Figures 5, 6 and 7 for long period, short period and single transit planet candidates.

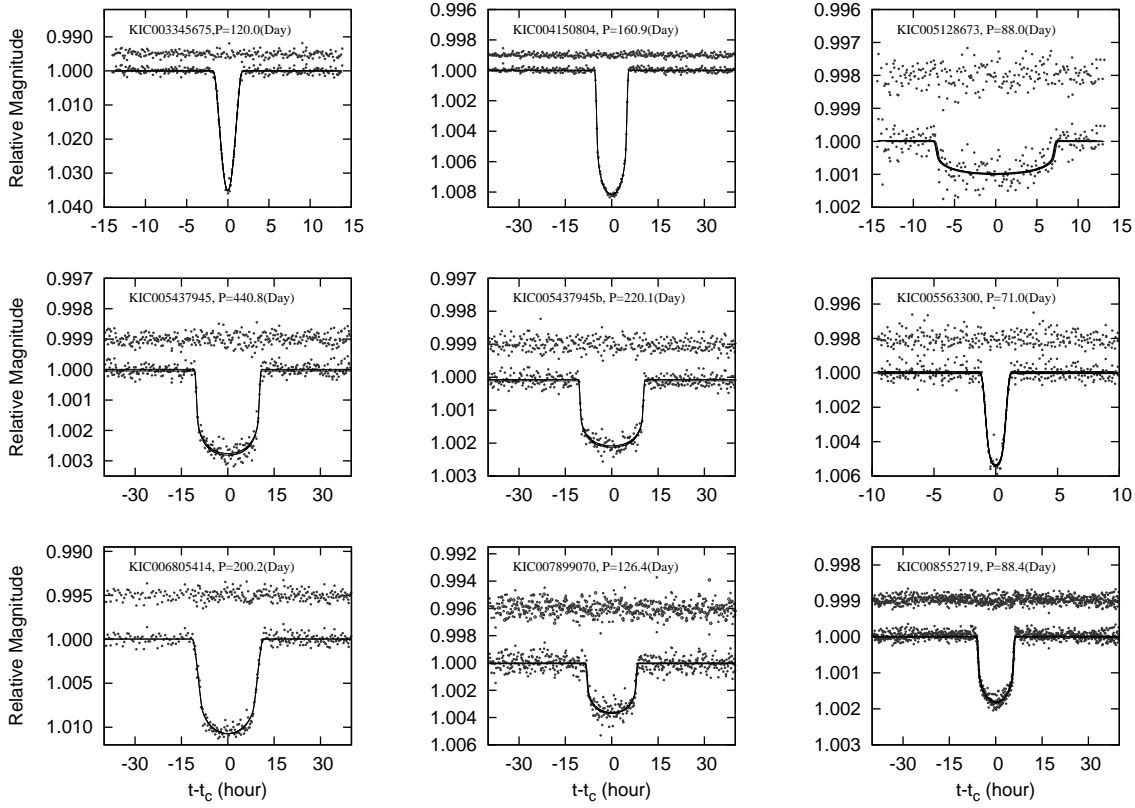


**Figure 5.** Long Period planet candidates. For each candidate we show the best-fit model on the phase-folded light curve (bottom of the panel) and the residuals (top of the panel). For each candidate, we model all transits separately. We then fold the transits using the locally computed transit centers.



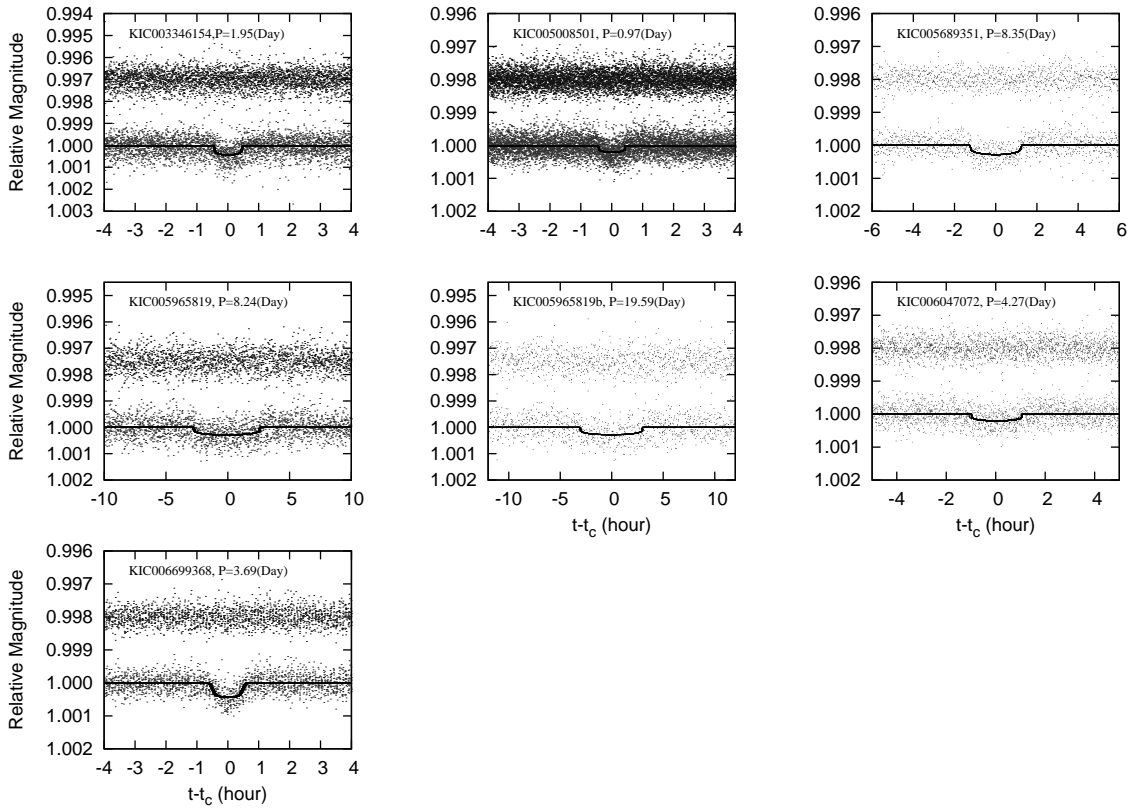


**Figure 6.** Short period planet candidates. For each candidate we show the best-fit model on the phase-folded light curve, together with the residuals from the fit (the configuration is the same as in Figure 5).

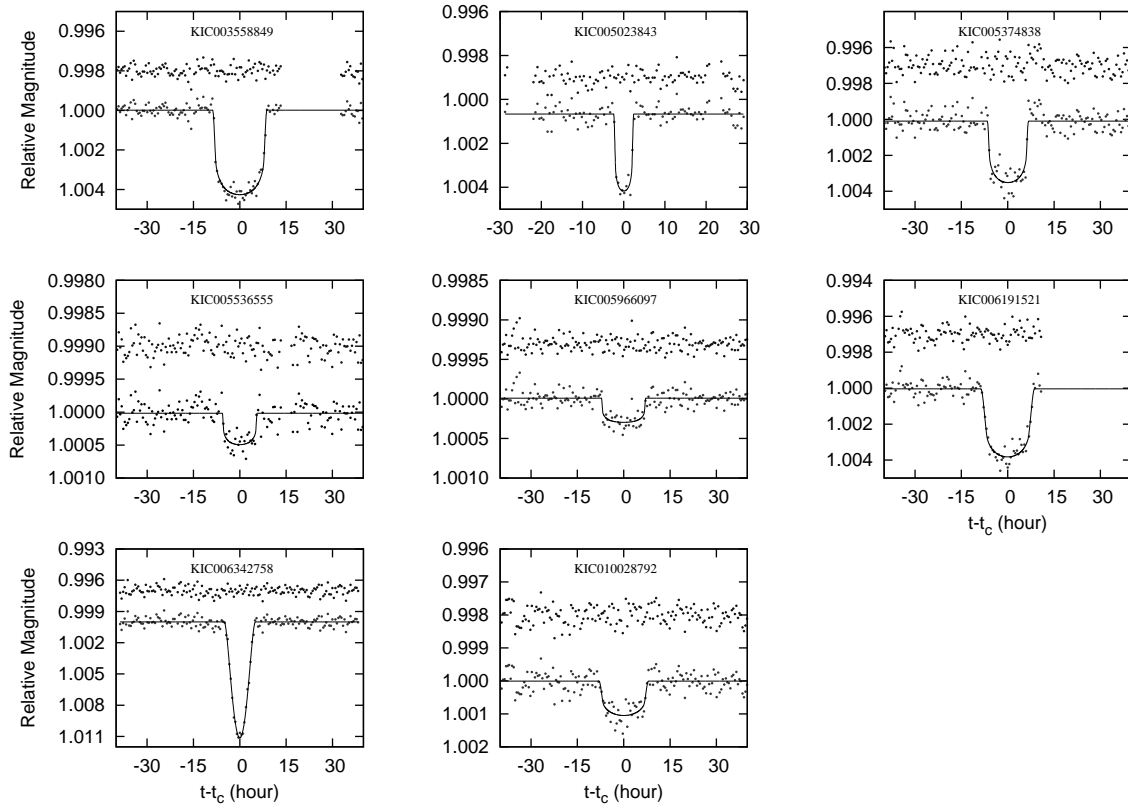


**Figure 7.** Single transit events. For each candidate we show the best-fit model on the light curve, together with the residuals from the fit (the configuration is the same as in Figure 5).

#### 4 CONCLUSIONS

We have analyzed 124840 stars with public *Kepler* data from quarters Q1–Q6 in total. We found 16 new planet candidates in this blind search. The periods of the new candidates range from  $\sim 0.968$  days to  $\gtrsim 440$  days. The estimated planetary radii vary from  $\sim 1.0 R_{\oplus}$  to  $14.73 R_{\oplus}$ . Nine of the planet candidates have sizes smaller than  $3 R_{\oplus}$ . We also found two new candidate multiple systems. In addition, we found one more planet candidate in the already known multiple planetary system KOI 505. We also detected 8 single transit events. Three of these have sizes smaller than  $3 R_{\oplus}$ . Two of the single transit events are found around stars with already identified planet candidates, indicating possible future new multiple systems. Seven new false positives are identified in our analysis of centroids variation. These findings demonstrate the importance of an independent search in the public data. Most of the *single* transit events (and a few of the planet candidates) were found by visual inspection of the light curves that were flagged by BLS. This suggests that combining automated searches, and visual inspection is an efficient approach for transiting planet searches.

Finally, we provide remarks on each of the new planet candidates below<sup>7</sup>.

**KIC 003345675:** 4 transit events with period of  $\sim 120$  days are found in the light curve. The transit signals are narrow and V-shaped, indicating a grazing geometry during eclipse. The depth of transit is  $\sim 0.038$  mag. However, the stellar radius is only  $0.6 R_{\odot}$ , indicating a possible  $14.73 R_{\oplus}$  size planet.

**KIC 003346154:** We identify a  $\sim 1.95$  day period planetary candidate in the system, with a planetary radius  $R_p \approx 1.7 R_{\oplus}$ .

**KIC 004150804:** The stellar parameters were not provided for this candidate in KIC. The transit signal has a long period of 160.88 days. There are only two complete transit events in the Q1–Q6 LC light curve. The transit in Q6 happened during the second earth point event in Q6; half of this transit can be found in the raw light curve during the recovery part of earth point. The radius of the planet candidate is expected to be 8% of the stellar radius. Follow-up observations on this host star would be important.

**KIC 005008501:** This planet candidate has a  $\sim 0.968$  day period. This is even shorter than the lower limit of our BLS search range (which is 1 day). The highest peak detected by BLS was  $\sim 1.93$  days. In the phase folded light curve with the 1.93 day period, however, we found two transit events during the visual inspection. The true period was then detected by applying a new BLS search in the period range of 2 hours to 3 days. According to the KIC, the radius of the host star is  $0.72 R_{\odot}$ . The modelled planet candidate size is  $1.20 \times 10^{-2} R_{\star} = 1.01 R_{\oplus}$ , almost that of Earth.

**KIC 005128673:** A super-Earth size ( $2.19 R_{\oplus}$ ) planet candidate with a period of 87.96 day. There are only four transit events in the light curve. One expected transit is lost between the transition from Q1 to Q2. The other expected

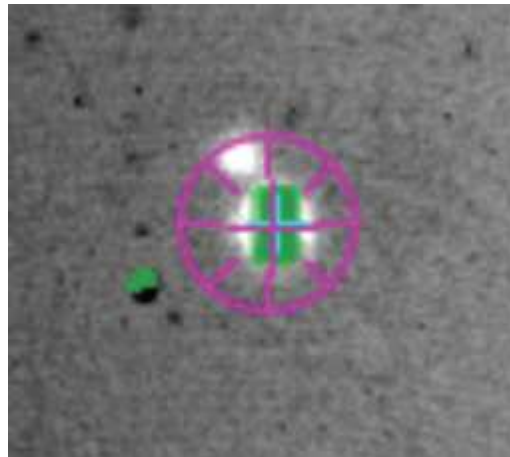


**Figure 8.** Image of the star KIC 5437945 taken with the APO 3.5 m Echelle slitviewer. The guider is centered on the star. A companion is resolved within  $\sim 5''$ .

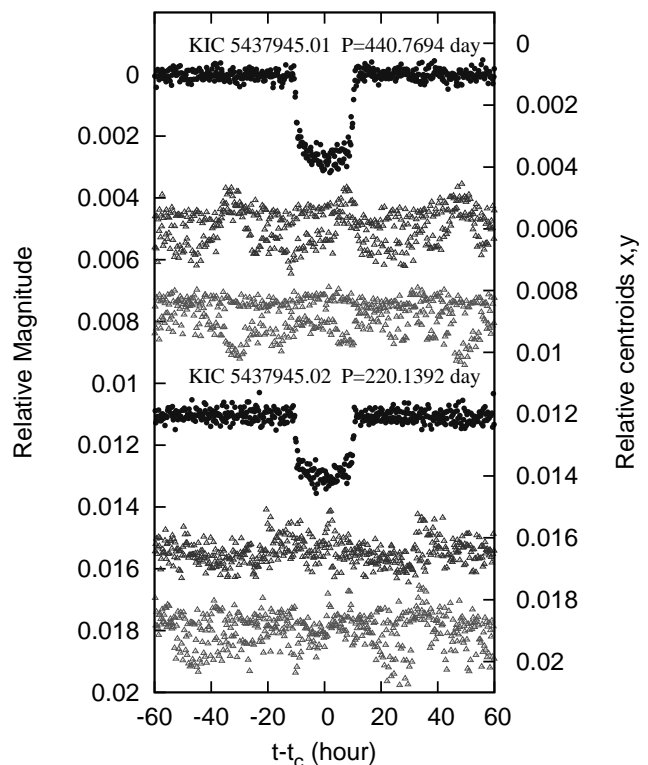


**Figure 9.** The two planet candidates of star KIC 5437954: from black to grey are the phased folded light curve, and the phased folded x and y direction centroids, all displayed separately. The upper (lower) three plots are for the first (second) planet candidate, with period  $P \sim 440(220)$  day. The centroids in the figure are the mean centroids after de-trending.

<sup>7</sup> The planet and stellar parameters we quote here are only approximated numbers for easy comparison. For accurate parameters and estimated errors, refer to Table 4.

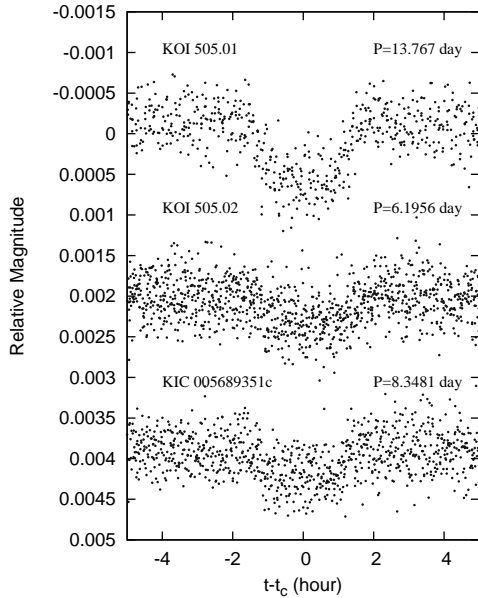


**Figure 10.** Folded de-trended light curve of KIC 005689351. Each transit is folded relative to its measured epoch, with the signal corresponding to the other two planet candidates removed from the light curve. The first two planet candidates with periods of  $\sim 13.767$  day and  $\sim 6.1956$  day have already been identified as KOI 505.01 (top) and KOI 505.02 (middle). We found a third planet candidate in the system with a period of 8.3481 day (bottom).

transit is lost in one of the Q2 coarse point gaps (between BJD 2455088.4 and BJD 2455089.3).

**KIC 005437945:** We identify four transit events in the light curve. The transit events in Q1 and Q6, and the ones in Q2 and Q5 share the same depths and durations, respectively. The former is modelled to be a  $7.5 R_{\oplus}$  planet candidates with 440 day period; the latter is modelled to be a  $6.4 R_{\oplus}$  planet candidate with a period of 220 days. A tweak happened during the transit in Q2 for the inner planet candidate, by carefully offsetting the magnitude on both sides of the tweak, we recover the full transit signal. We resolved a faint close companion ( $\sim 5''$ ) in the Echelle slitviewer of the APO 3.5 m telescope (See Figure 8. We examined 2MASS image stamps in J,H and K and DSS 1,2 images in red and blue. All of the above show that the companion is bluer than KIC 005437945, which indicates that it is unlikely to be a physically associated companion. We present the phase folded de-trended centroid for both planet candidates in Figure 9. No anomalous motion is shown in either direction during transit.

**KIC 005563000:** A  $10.22 R_{\oplus}$  size planet candidate with a 71 day period. All seven transit events in Q1-Q6 are detected and modelled. However, we expect the next transit would be lost in the transition between Q6 and Q7.

**KIC 005689351:** We identify a  $2.2 R_{\oplus}$  planet candidate with a period of 8.348 day in the system, which already has 2 KOIs. The folded light curve of the three planet candidates are separately shown in Figure 10. When modeling one planet candidate, we make use of the detected periods and epochs to filter out the transit signals due to the other two. The top and middle panels present the two KOIs, with

periods 13.767 day and 6.1956 day. The third planet candidate we found is in a 4:3 resonance with the latter. This is the first reported 3:4:6 resonance 3-planet candidate system. Rein et al. (2012) suggests that a resonance chain of three or more planets, in analog to Jupiter’s moon system, would overcome the difficulties of forming the 4:3 resonance in the traditional way. This system provides an interesting testing-ground for the theory.

**KIC 005965819:** We found two planet candidates in the system, both with modelled radii less than  $2 R_{\oplus}$ . The inner planet candidate orbits the host star with a period of 8.2 days; the outer planet candidate has a 19.6 day period. They are not in a tight resonance with each other. We note that the transit durations of these two planet candidates are longer than the values expected assuming circular orbits. This might indicates the planets are in eccentric orbits or the stellar radius of KIC 005965819 is in fact larger that what is provided by KIC.

**KIC 006047072:** A  $1.33 R_{\oplus}$  size planet candidate, with 4.27 day period.

**KIC 006699308:** A  $2.41 R_{\oplus}$  size planet candidate, with 3.69 day period.

**KIC 006805414:** We found two identical transit events in the light curve (Q3 and Q5), indicating the period is 200.23 day. The modelled planet size is  $9.3 R_{\oplus}$ .

**KIC 007899070:** A long period (126.43 day) super earth candidate with a size of  $2.85 R_{\oplus}$ . The host star has a radius of  $0.49 R_{\odot}$ .

**KIC 008552719:** A Neptune size planet with  $\sim 88.4$  day period. We note that in the *Kepler* PDC (Pre-search data conditioning) flux there is a 0.03 magnitude flux tweak in Q2 (duration  $\sim 2$  hours), which might mask the transit signal in their transit analysis process.

Table 1. Anomaly Summary Table

Start(BJD-2454000)	End(BJD-2454000)	Quarter	Anomaly Type
1002.5198	1002.7241	2	EXCLUDE <sup>a</sup>
1014.5146	1016.7214	2	SAFE MODE <sup>b</sup>
1033.2932	1033.3341	2	TWEAK <sup>c</sup>
1056.4853	1056.8313	2	COARSE POINT <sup>d</sup>
1063.2896	1064.3726	2	EARTH POINT <sup>e</sup>
1073.3632	1073.3632	2	ARGABRIGHTENING <sup>f</sup>
1079.1866	1079.1866	2	TWEAK
1080.8008	1080.8212	2	ARGABRIGHTENING
1088.4018	1089.3213	2	COARSE POINT
1093.2239	1093.2239	3	EARTH POINT
1100.4163	1100.5389	3	COARSE POINT
1104.5233	1104.5438	3	COARSE POINT
1113.4116	1117.3346	3	MEMORY ERROR <sup>g</sup>
1123.5461	1124.4248	3	EARTH POINT
1206.2584	1206.2584	4	TWEAK
1216.4137	1217.3128	4	EARTH POINT
1229.8386	1233.8231	4	SAFE MODE
1307.9995	1309.2869	5	-
1336.7713	1337.6091	5	-
1399.5042	1400.3828	6	EARTH POINT
1431.2374	1432.1978	6	EARTH POINT

<sup>a</sup> EXCLUDE: manually excluded cadence before pipeline processing.

<sup>b</sup> SAFE MODE: due to unanticipated sensitivity to cosmic radiation, or unanticipated responses to command sequences. The amplitude of flux is affected after the end date of safe mode, data for additional 3 days are removed rather than corrected. Data on both side are offset in magnitude to ensure continuity by a polynomial fit.

<sup>c</sup> TWEAK (Attitude Tweaks): discontinuities in the data due to small attitude adjustments. The discontinuities are corrected by offset data on both side according to a polynomial fit.

<sup>d</sup> COARSE POINT (Loss of Fine Pointing): due to losing fine pointing control, removed.

<sup>e</sup> EARTH POINT: change of attitude due to monthly data downlink. Affect data the same way as safe mode. Corrected by the same method as safe mode.

<sup>f</sup> ARGABRIGHTENING: diffuse illumination of the focal plane. Removed. Only argabrightening events longer than one cadence is listed here.

<sup>g</sup> MEMORY ERROR: due to onboard spacecraft errors, gapped by the pipeline, the continuity on both end of gap is checked. Only memory errors longer than one cadence is listed here.

<sup>h</sup> The format of data release handbook 8 for Q5 data is different from other quarters. There is no safe mode, tweak, coarse point and exclude phenomena in Q5, only listed two big gaps possibly due to earth point here.

Table 2. False Positive List

Star	Kepmag	RA (deg)	Dec (deg)	Epoch (BJD-2454000)	Period (day)	Depth x <sup>b</sup> (Pixel)	Depth y <sup>b</sup> (Pixel)	SNR
KIC003336765	13.617	19.330387	38.463631	965.1613	1.84483	-	-0.00032	38.93
KIC004072333	15.664	19.688677	39.162540	965.5638	2.00775	-	0.0030	37.69
KIC005443775	12.936	19.355742	40.653061	967.8765	3.30754	-	-0.00034	73.09
KIC005565497 <sup>c</sup>	11.521	19.958805	40.758141	966.11575	1.412532	-0.0126	-0.0011	131.4
KIC005649325 <sup>c</sup>	13.560	19.932024	40.87204	1196.35	195.63	0.0016	-	7.81
KIC007906739 <sup>c</sup>	13.601	19.786779	43.654259	969.868	7.0151	0.0012	-0.0019	21.33
KIC007989422 <sup>c</sup>	11.539	20.015013	43.758179	966.414	7.4776	-	-0.0026	26.92

<sup>a</sup> We only reported the false positives not in the *Kepler* FP catalog here. We do not report FPs in *single* transit events. These FPs are all identified by examining the centroids. We refer to the text for a detailed description of the method.

<sup>b</sup> Depth is computed from the phase folded centroids. Both x and y direction are presented. We do not list a depth when the shift is not detected.

<sup>c</sup> There are visible companion(s) in the 2MASS image stamp within  $20'' \times 20''$ .

Table 3. Stellar Parameter Table

Star	Kepmag	$R_*$ ( $R_\odot$ )	$T_{\text{eff}}$ (K)	$\log g$ (cgs)	[Fe/H]	$u_a$ <sup>b</sup>	$u_b$ <sup>c</sup>
003345675	15.635	0.598	4105	4.620	0.137	0.57	0.17
003346154	14.575	0.957	5513	4.490	0.118	0.45	0.22
004150804 <sup>d</sup>	12.888	-	-	-	-	0.40	0.25
005008501	14.479	0.715	6311	4.759	0.110	0.32	0.31
005128673	14.000	0.751	5585	4.689	-0.196	0.41	0.25
005437945	13.771	1.466	6093	4.172	-0.374	0.32	0.30
005563300	14.710	1.223	5090	4.270	-0.125	0.52	0.18
005689351	14.194	1.259	4985	4.242	0.238	0.57	0.14
005965819	15.024	0.981	5718	4.481	-0.066	0.40	0.26
006047072	14.553	0.906	5683	4.544	-0.193	0.39	0.26
006699368	14.336	1.105	5859	4.389	-0.177	0.36	0.28
006805414	15.392	0.894	5802	4.559	-0.081	0.38	0.27
007899070	15.500	0.497	5428	4.997	-0.234	0.44	0.24
008552719	12.160	0.822	5114	4.579	0.015	0.53	0.17
003558849	14.218	1.052	5938	4.432	-0.410	0.33	0.30
005023843	14.942	1.034	6235	4.457	-1.592	0.27	0.32
005374838	15.469	1.035	5832	4.442	-0.156	0.37	0.28
005536555	13.465	0.962	5720	4.497	-0.476	0.35	0.28
005966097	12.352	1.512	6223	4.151	-1.427	0.28	0.31
006191521	15.201	0.875	5469	4.559	-0.573	0.39	0.27
006342758	14.586	0.878	4973	4.515	0.174	0.57	0.14
010028792	14.600	0.854	5537	4.583	-0.072	0.43	0.24

<sup>a</sup> We use a double line in the middle of table to divide periodic planetary candidates (above the line) and single transit events (below the line).

<sup>b</sup> The quadratic limb darkening parameter a.

<sup>c</sup> The quadratic limb darkening parameter b.

<sup>d</sup> The limb darkening coefficient is obtained by fitting with J, H and K color.

Table 4. Planet Candidates Table

KIC	Epoch (BJD-2454000)	$\sigma_E$ ( $10^{-3}$ )	Period (day)	$\sigma_P$ ( $10^{-4}$ )	$R_p$ ( $R_\odot$ )	$R_p/R_*$	$\sigma_R$ ( $10^{-3}$ )	$b$	$\zeta/R_*$ ( $day^{-1}$ )	SNR	DSP	$\chi^2$
003345675	1203.14403	0.12	120.002673	0.80	0.13506	0.22586	0.28	$0.90 \pm 0.00$	$26.70 \pm 0.000$	38.93	3.88	18.34
003346154	1231.72962	0.31	1.9527041	0.057	0.01701	0.01777	0.78	$0.48 \pm 0.20$	$53.7 \pm 1.1$	64.37	17.83	4.40
004150804	1271.38683	0.69	160.8818	10	-	0.07985	0.64	$0.365 \pm 0.080$	$4.801 \pm 0.013$	23.75	6.89	0.35
005008501	1073.17351	0.38	0.9680371	0.023	0.00922	0.01290	0.63	$0.65 \pm 0.18$	$55.4 \pm 1.3$	10.95	24.61	1.83
005128673 <sup>c</sup>	1353.1823	5.2	87.9654	36	0.02062	0.02746	0.44	$0.1435 \pm 0.0049$	$3.368 \pm 0.048$	10.83	8.32	2.81
005437945 <sup>c</sup>	1413.1318	2.5	440.7694	36	0.06900	0.04707	0.60	$0.40 \pm 0.13$	$2.342 \pm 0.010$	-	-	0.37
005437945b <sup>c</sup>	1299.1193	3.0	220.1392	44	0.05890	0.04018	0.56	$0.39 \pm 0.14$	$2.333 \pm 0.012$	10.14	11.18	0.97
005563300	1180.89946	0.54	71.05483	1.7	0.0936	0.0766	1.1	$0.870 \pm 0.011$	$26.93 \pm 0.28$	20.99	5.286	4.16
005689351 <sup>b</sup>	1178.5459	1.3	8.348078	0.74	0.0201	0.0160	1.3	$0.71 \pm 0.51$	$19.50 \pm 0.52$	17.06	11.69	1.72
005965819	1349.7889	1.7	8.23994	0.10	0.01510	0.01539	0.89	$0.39 \pm 0.24$	$9.07 \pm 0.13$	53.23	17.63	3.50
005965819b	1251.9257	4.3	19.59154	4.1	0.01508	0.01537	0.80	$0.63 \pm 0.17$	$7.84 \pm 0.31$	17.42	14.36	3.52
006047072	1188.2349	2.3	4.270998	0.42	0.0122	0.0135	1.3	$0.71 \pm 0.37$	$23.8 \pm 1.4$	16.64	8.51	1.96
006699368	1256.07682	0.62	3.690306	0.21	0.0221	0.0200	1.5	$0.82 \pm 0.15$	$47.3 \pm 1.8$	16.64	8.51	1.60
006805414	1338.68304	0.89	200.2347	12	0.08532	0.09544	0.30	$0.635 \pm 0.011$	$2.430 \pm 0.004$	12.67	11.38	9.19
007899070 <sup>c</sup>	1252.3924	1.2	126.4380	12	0.02616	0.05264	0.45	$0.26 \pm 0.12$	$2.992 \pm 0.010$	21.54	29.13	7.18
008552719 <sup>c</sup>	1274.4928	2.4	88.40759	9.3	0.0317	0.0386	1.2	$0.58 \pm 0.12$	$4.141 \pm 0.027$	38.30	16.51	0.31
003558849	1112.9840	1.5	-258	-	0.06119	0.05817	0.61	$0.34 \pm 0.12$	$2.919 \pm 0.013$	-	-	2.11
005023843	1320.7241	1.2	-358	-	0.0561	0.0543	1.5	$0.3 \pm 1.0$	$11.00 \pm 0.15$	-	-	2.83
005374838	1293.2325	1.4	-332	-	0.05353	0.05172	0.59	$0.30 \pm 0.13$	$3.839 \pm 0.021$	-	-	6.22
005536555	1325.409	11	-365	-	0.0186	0.0193	1.1	$0.374 \pm 0.024$	$4.48 \pm 0.22$	-	-	0.72
005966097	1449.623	26	-489	-	0.0246	0.0163	1.5	$0.68 \pm 0.19$	$3.45 \pm 0.30$	-	-	0.20
006191521 <sup>b</sup>	1215.9432	2.1	-253	-	0.0511	0.0584	1.2	$0.747 \pm 0.049$	$3.143 \pm 0.026$	-	-	4.63
006342758	1386.89511	0.79	-428	-	0.1145	0.1304	5.6	$0.934 \pm 0.010$	$8.66 \pm 0.54$	-	-	4.17
010028792 <sup>b</sup>	1119.0854	6.6	-347	-	0.0255	0.0299	1.7	$0.66 \pm 0.16$	$3.293 \pm 0.077$	-	-	2.09

<sup>a</sup> We use a double line in the middle of table to divide periodic planetary candidates (above the line) and single transit events (below the line).

<sup>b</sup> Stars already identified as KOIs. The candidates presented here are transit signals that have not previously been detected in these systems.

<sup>c</sup> Systems may be blended by nearby stars. There exists a visible companion(s) within 20 square arcseconds in a 2MASS image stamp centered on the target star.



**ACKNOWLEDGMENTS**

We thank the *Kepler* team for the high quality public data. This research was partly support from NSF grant AST-1108686.

**REFERENCES**

- Ahmed, N. T., Natarajan, T. K. R., & Rao, K. R. 19 74, IEEE Trans. Computers, 90
- Bakos, G., Noyes, R. W., Kovács, G., et al. 2004, PASP, 116, 266
- Bakos, G. Á., Torres, G., Pál, A., et al. 2010, ApJ, 710, 1724
- Bakos, G. Á., Hartman, J. D., Torres, G., et al. 2011, Detection and Dynamics of Transiting Exoplanets, St. Michel l'Observatoire, France, Edited by F. Bouchy; R. Díaz; C. Moutou; EPJ Web of Conferences, Volume 11, id.01002, 11, 1002
- Batalha, N. M., Rowe, J. F., Bryson, S. T., et al. 2012, arXiv:1202.5852
- Borucki, W. J., Koch, D., Basri, G., et al. 2010, Science, 327, 977
- Borucki, W. J., Koch, D. G., Basri, G., et al. 2011, ApJ, 728, 117
- Borucki, W. J., Koch, D. G., Basri, G., et al. 2011, ApJ, 736, 19
- J. L. Christiansen, T. Barclay, J. M. Jenkins, et al., 2012, Kepler Data Release 14 Notes (KSCI-19054-001).
- J. L. Christiansen, J. E. Van Cleve, J. M. Jenkins, et al., 2012, Kepler Data Characteristics Handbook (KSCI-19040-003).
- Fischer, D. A., Schwamb, M. E., Schawinski, K., et al. 2012, MNRAS, 419, 2900
- Ford, E. B., Ragozzine, D., Rowe, J. F., et al. 2012, arXiv:1201.1892
- Gilliland, R. L., Jenkins, J. M., Borucki, W. J., et al. 2010, ApJ, 713, L160
- Holman, M. J., Winn, J. N., Latham, D. W., et al. 2006, ApJ, 652, 1715
- Jenkins, J. M., Caldwell, D. A., Chandrasekaran, H., et al. 2010, ApJ, 713, L87
- Jenkins, J. M., Caldwell, D. A., Chandrasekaran, H., et al. 2010, ApJ, 713, L120
- Kipping, D. M. 2008, MNRAS, 389, 1383
- Kipping, D., & Bakos, G. 2011, ApJ 733, 36
- Kipping, D. M., & Spiegel, D. S. 2011, MNRAS, 417, L88
- Kovács, G., Zucker, S., & Mazeh, T. 2002, A&A, 391, 369
- Kovács, G., Bakos, G., & Noyes, R. W. 2005, MNRAS, 356, 557
- Koch, D. G., Borucki, W. J., Basri, G., et al. 2010, ApJ, 713, L79
- Lintott, C. J., Schawinski, K., Slosar, A., et al. 2008, MNRAS, 389, 1179
- Lintott, C., Schwamb, M. E., Sharzer, C., et al. 2012, arXiv:1202.6007
- Loeb, A., & Gaudi, B. S. 2003, ApJ, 588, L117
- P. Machalek, J. L. Christiansen, J. E. Van Cleve, et al., 2011, Kepler Data Release 9 Notes (KSCI-19049-001).
- P. Machalek, J. L. Christiansen, J. E. Van Cleve, et al., 2010, Kepler Data Release 8 Notes (KSCI-19048-001).
- Mandel, K., & Agol, E. 2002, ApJ, 580, L171
- Mazeh, T., & Faigler, S. 2010, A&A, 521, L59
- Murphy, S. J. 2012, MNRAS, 2509
- Pál, A., Bakos, G. Á., Torres, G., et al. 2008, ApJ, 680, 1450
- Prša, A., Batalha, N., Slawson, R. W., et al. 2011, AJ, 141, 83
- Rein, H., Payne, M. J., Veras, D., & Ford, E. B. 2012, arXiv:1204.0974
- Sing, D. K. 2010, A&A, 510, A21
- Smith, J. C., Stumpe, M. C., Van Cleve, J. E., et al. 2012, arXiv:1203.1383
- Steffen, J. H., Fabrycky, D. C., Ford, E. B., et al. 2012, MNRAS, 421, 2342